CHAPTER 7

MELNIKOV PROCESSES AND NOISE-INDUCED ESCAPES: APPLICATIONS TO ENGINEERING, PHYSICS, AND BIOLOGY

M. Franaszek[1], *M. Frey*[2] *and E. Simiu*[1]

[1]Building and Fire Research Laboratory
National Institute of Standards and Technology
Gaithersburg, MD 20899, USA

[2]Department of Mathematics, Bucknell University
Lewisburg, PA 17837, USA

For a class of deterministic systems the necessary condition for chaos is that the system's Melnikov function have simple zeros. The behavior of those systems' stochastic counterparts is similarly characterized by their Melnikov processes. We summarize: (1) recent research by the authors on the use of Melnikov processes to obtain weak upper bounds for rates of escape from a potential wall induced by a variety of types of noise, including dichotomous noise, and (2) applications of Melnikov processes in oceanography, the investigation of column snap-through induced by stochastic loads, nonlinear control, stochastic resonance, and the behavior of auditory nerve fibers.

1. Introduction

Chaotic dynamics theory and its applications were until recently concerned primarily with deterministic systems. In this paper we examine applications of chaotic dynamics to a wide class of stochastic dynamical systems.

Deterministic multistable systems excited harmonically can have chaotic motions featuring irregular escapes. Chaotic motions in such deterministic systems and motions in those systems' stochastically excited counterparts can be virtually indistinguishable visually (Simiu and Frey, 1996a). More importantly, those motions have common mathematical properties allowing the application to the stochastic systems of an approach originally developed for the deterministic case: the Melnikov approach. This is a consequence of (1) Wiggins' (1988) result that systems capable of chaotic behavior under harmonic excitation can also behave chaotically if the excitation is quasiperiodic, and (2) the application of this result to systems excited by physically realizable stochastic processes, which can be approximated arbitrarily closely by random quasiperiodic sums (Frey and Simiu, 1993). For stochastic systems the Melnikov approach -- referred to as the stochastic Melnikov approach -- is useful in problems involving escapes.

The purpose of this paper is to provide a summary of recent research performed by the authors on the stochastic Melnikov approach. The techniques we use are based on Melnikov conditions for the occurrence of chaos. For both deterministic and stochastic systems these conditions are necessary but not sufficient. Results yielded by the Melnikov approach are therefore weak, though less so for transient than for steady state motions. For example, for a buckled column excited harmonically at a given frequency, the Melnikov approach yields the excitation amplitude below which escapes (i.e., snap-through) cannot occur. Numerical simulations show, however, that steady state snap-through is not observed unless that amplitude is exceeded by a factor of, say, two.

Such limitations notwithstanding, the Melnikov approach is a useful addition to the

Stochastically Excited Nonlinear Ocean Structures. Chapter 7, World Scientific, NJ, Shlesinger, M. F.; Swean, T., Editors, 187-212 pp, 1998.

array of existing nonlinear dynamics tools insofar as it can yield qualitative results and insights into the behavior of multistable systems that may not be obtainable by other means. This is all the more true as the Melnikov approach, which in theory is valid only for systems with asymptotically small damping and excitation, turns out in practice to be applicable even when the damping and excitation are relatively large.

An overview of Melnikov theory for a class of planar harmonically, quasiperiodically and stochastically excited systems is presented in Section 2. Section 3 presents results on upper bounds for escape rates obtained by the stochastic Melnikov approach. Sections 4 through 9 discuss applications to physical, engineering and biological systems.

2. Overview of the Melnikov Approach

2.1 Unperturbed Integrable Systems With Homoclinic or Heteroclinic Orbits. Perturbed Systems. Persistence Theorem. Melnikov Distance

The phase plane diagrams of a wide class of frictionless and unforced planar multistable systems have one or more hyperbolic saddle points from which nongeneric orbits emanate in forward and reverse time. These orbits form a separatrix between regions of the phase plane. The separatrix is impermeable, that is, motions starting inside (outside) the separatrix stay inside (outside) it for all time. The nongeneric orbits are typical of Hamiltonian multistable systems and are called *homoclinic* or *heteroclinic* depending upon whether they join saddle points that coincide or are distinct.

The evolution of a planar system may also be represented in a three-dimensional phase space with orthogonal coordinate axes Ox, $O\dot{x}$, Ot. A homoclinic orbit can be interpreted in that space as the intersection with a plane of section $t=const$ of (1) the surface consisting of the set of all trajectories that approach the axis $\Gamma_0=Ot$ asymptotically in forward time, and (2) the surface consisting of the set of all trajectories that approach Ot in reverse time. These surfaces are the *stable manifold* and the *unstable manifold*, respectively. Similar definitions apply to the heteroclinic case. Like their intersections with a plane of section $t=const$, the stable and unstable manifold coincide.

Assume the system is subjected to a perturbation of order $\epsilon \ll 1$. If the perturbation is bounded and sufficiently smooth, it follows from the *persistence theorem* that the line $\Gamma_0 \equiv Ot$ persists under perturbation as a smooth curve $\Gamma_\epsilon=\Gamma_0+O(\epsilon)$, and that the perturbed system has a stable manifold and an unstable manifold contained in an $O(\epsilon)$ neighborhood of the unperturbed manifolds. The perturbed stable and unstable manifolds are the surfaces consisting, respectively, of the sets of all trajectories that approach Γ_ϵ asymptotically in forward time and that approach Γ_ϵ asymptotically in reverse time.

Owing to the perturbation, the stable and unstable manifolds no longer coincide. The *Melnikov distance* is the distance between the separated stable and unstable manifolds, measured along a line normal to the unperturbed manifolds.

2.2 Perturbed Systems with Harmonic Excitation. Melnikov Functions. Necessary Condition for Chaos

We now consider the system

$$\ddot{x} = -V'(x) + \epsilon[G(t) - \beta\dot{x}] \tag{1}$$

and assume that the perturbation is $G(t) = \gamma\cos(\omega t)$ and $V(x)$ is a multi-well potential. It can be shown that, to first order, the Melnikov distance is proportional to the *Melnikov function*. Under certain conditions (Wiggins, 1988), for the system and assumptions under consideration the Melnikov function has the expression

$$M(\tau_o, t') = -\beta c + \gamma S(\omega)\sin\omega(\tau_o + t') \tag{2}$$

where the constant c and the *Melnikov scale factor* $S(\omega)$ depend on the homoclinic orbit, and τ_0 and t' are time coordinates defining the position of a point on the unperturbed manifolds. For sufficiently small ϵ, if the Melnikov function has simple zeros, the stable and unstable manifolds of the perturbed system intersect transversely. If the Melnikov function is bounded away from zero the stable and unstable manifolds do not intersect. For Eq. 2 the condition for transverse intersection

$$\gamma S(\omega) > \beta c. \tag{3}$$

The traces of intersecting stable and unstable manifolds on a plane of section form a *homoclinic tangle*, exhibiting *lobes* defined by segments of the homoclinic tangle, and a curve, called *pseudoseparatrix*, consisting of the union of segments that most closely approximates the homoclinic or heteroclinic orbit of the unperturbed system. Transport from the inside to the outside of the pseudoseparatrix and vice-versa is effected by *turnstile lobes* (Wiggins, 1992). The mapping of ceratin areas of the phase plane by the nonlinear dynamical system entails *expansion, contraction* and *folding* leading to geometrical structures that may be studied by symbolic dynamics techniques. Associated with such structures are trajectories that may be *sensitive to initial conditions*, and therefore imply the existence of a positive *Lyapounov exponent*. The *Smale-Birkhoff theorem* states that for a harmonically excited planar system to be chaotic its Melnikov function must have have simple zeros (Melnikov necessary condition for chaos).

Unlike the separatrix of an unperturbed system, which is impermeable in the sense that it cannot be crossed by any orbit, a pseudoseparatrix can be permeable. This allows the occurrence of chaotic motions featuring escapes from a preferred region. The mechanism by which such motions occur is associated with the action of the lobes and is referred to as *chaotic transport* through a pseudoseparatrix. Since chaotic motions with escapes are a form of chaotic behavior, it is clear that they cannot occur unless the Melnikov necessary condition for chaos (i.e., Eq. 3) is satisfied.

2.3 *Perturbed Systems With Quasiperiodic Excitation. Generalized Melnikov Functions*

It can be shown that, if in Eq. 1 the excitation $G(t)$ is quasiperiodic; that is, if

$$G(t) = \sum_{i=1}^{N} \gamma_i\cos(\omega_i t + \theta_{oi}) \tag{4}$$

then the Melnikov distance is proportional, to first order in ϵ, to the *generalized Melnikov function* (a term used by Beigie et al., 1991)

$$M(\tau_0,t') = -\beta c + \sum_{i=1}^{N} \gamma_i S(\omega_i)\sin[\omega_i(\tau_0+t')+\theta_{0i}] \tag{5}$$

For small perturbations the stable and unstable manifolds intersect transversely if the generalized Melnikov function has simple zeros, that is, if

$$\sum_{i=1}^{N} \gamma_i S(\omega_i) > \beta c \tag{6}$$

By virtue of a simple extension of the Smale-Birkhoff theorem (Beigie et al., 1991), Eq. 6 is the Melnikov necessary condition for chaos in quasiperiodically excited systems (1).

2.4 Perturbed Systems With Stochastic Excitation. Melnikov Processes

The extension to stochastically excited systems of results obtained for the quasiperiodic excitation case follows from the fact that physically realizable stochastic processes can be approximated as closely as desired by quasiperiodic sums with random parameters.

We illustrate this statement for a process $G(t)$ with Gaussian distribution, unit variance, and one-sided spectral density $2\pi\Psi_0(\omega)$. Such a process can be approximated by the Shinozuka representation $G(t) \simeq G_N(t)$, where

$$G_N(t) = (2/N)^{1/2} \sum_{i=1}^{N} \cos(\omega_i t + \phi_i) \tag{7}$$

where $\{\omega_i;\ i=1,2,..,N\}$ and $\{\phi_i;\ i=1,.2,..,N\}$ are independent identically distributed nonnegative random variables with probability density Ψ_0 and uniform distribution over the interval $[0,2\pi]$, respectively. The parameter N of the model is finite, although if necessary it can be arbitrarily large. It is easy to show that the spectral density of $G_N(t)$ is $2\pi\Psi_0(\omega)$, that is, the same as that of $G(t)$. Other approximate representations of stochastic processes are available -- see, e.g., Rice (1954).

The ensemble of Melnikov functions induced by a stochastic process $G(t)$ is referred to as a *Melnikov process* (Simiu, 1996; Simiu and Frey, 1996). Since a Gaussian excitation process is unbounded, one of the requirements for the proof of the persistence theorem is not satisfied. No Melnikov process can therefore be associated with a Gaussian excitation. However, the Melnikov process is defined if the excitation process can be assumed to have the form of $G_N(t)$, which is nearly Gaussian. We therefore use in the expression for the Melnikov process the near-Gaussian process $G_N(t)$ instead of the strictly Gaussian process $G(t)$. This is justified by the following fact. Physical processes

to which a Gaussian model is applied have marginal distributions induced by a finite -- albeit large number -- of contributions, rather than by an infinite number as is assumed in the central limit theorem. If in Eq. 1 $G(t)$ is a Gaussian distribution, substitution of the approximation $G_N(t)$ for $G(t)$ yields an expression for the Melnikov process similar to Eq. 5. The expectation and spectral density of the Melnikov process can be shown to be, respectively,

$$E[M_N(t)] = -\beta c, \qquad \Psi_{MN}(\omega) = 2\pi\gamma^2 S^2(\omega)\Psi_o(\omega) \tag{8a,b}$$

(Frey and Simiu, 1993). Knowledge of the spectral density allows the estimation of the mean time between consecutive zero upcrossings for the Melnikov process, τ_u. Simple chaotic transport considerations can then be used to show that τ_u is a weak lower bound for the system's mean escape time τ_e (Simiu, 1996; Simiu and Frey, 1996). As shown in the next section, under certain conditions weak lower bounds can be obtained for the probability that no escapes will occur during a specified time interval. Melnikov processes induced by other types of stochastic processes, for example white noise or dichotomous noise, can similarly be defined (Simiu and Frey, 1996b).

3. Melnikov Processes and Escapes from Preferred Regions of Phase Space

3.1 Chaotic Behavior and Escapes

The result that motion in near-integrable systems with escapes induced by Gaussian excitations is sensitive to initial conditions is a consequence of the Smale-Birkhoff theorem and is relatively recent (Frey and Simiu, 1993).

We mentioned that, for a class of near-integrable deterministic planar systems with quasiperiodic excitation, escapes from a potential well are associated with the mechanism of chaotic transport across the pseudoseparatrix. The same mechanism is at work for those systems' stochastically excited counterparts, since each of the realizations of the stochastic excitation can be approximated by a quasiperiodic function. As in the deterministic case, a phase space slice through the stable and unstable manifolds induced by a realization of its stochastic excitation has a pseudoseparatrix, entraining and detraining lobes, and turnstile lobes.

3.2 Condition Guaranteeing the Non-occurrence of Chaos in Systems Excited by Finite-tailed Stochastic Processes. Example: Dichotomous Noise

Melnikov processes induced by finite-tailed random excitations (i.e., by random processes whose marginal distributions have finite tails) are also finite-tailed. Therefore, parameter regions exist for which the Melnikov necessary condition for chaos can never be satisfied. A criterion guaranteeing the nonoccurrence of chaos and, *a fortiori*, of chaotic exits from a well, can be derived from the requirement that the system parameters be contained in those parameter regions. As an example (Sivathanu, Hagwood and Simiu, 1995), we consider the perturbed standard Duffing-Holmes equation

$$\dot{x}_1 = x_2 \tag{9a}$$

$$\dot{x}_2 = x_1 - x_1^3 + \epsilon[\gamma G(t) - \beta x_2)] \tag{9b}$$

($\beta > 0$, $0 < \epsilon \ll 1$), where $G(t)$ is the coin-toss square wave dichotomous noise process

$$G(t) = a_n, \qquad [\alpha + (n-1)]t_1 < t \leq (\alpha + n)t_1, \tag{10}$$

n is the set of integers, the random variable α is uniformly distributed between 0 and 1, the independent random variables a_n take on the values -1 and 1 with probabilities 1/2 and 1/2, respectively, and t_1 is a parameter of $G(t)$. Let $G_\epsilon(t)$ be an approximation to $G(t)$ consistent with persistence theorem requirements. For a system with $\dot{x}_h(-t) \equiv h(t)$, where $x_h(t)$ is the abscissa of the homoclinic orbit, the Melnikov process due to $G_\epsilon(t)$ is

$$M_\epsilon(\tau_0, t') = \int_{-\infty}^{\infty} h(\xi) G_\epsilon(\tau_0 + t' - \xi) d\xi - 4\beta/3 \tag{11a}$$

$$= \int_{-\infty}^{\infty} h(\xi)\{G(\tau_0 + t' - \xi) - [G(\tau_0 + t' - \xi) - G_\epsilon(\tau_0 + t' - \xi)]\} d\xi - 4\beta/3. \tag{11b}$$

Since the contribution of the difference $G(\tau_0 + t' - \xi) - G_\epsilon(\tau_0 + t' - \xi)$ to the integral of Eq. 12b can be made as small as desired, we can write $M_\epsilon(\tau_0, t') \approx M(\tau_0, t')$ where, formally,

$$M(\tau_0, t') = \int_{-\infty}^{\infty} h(\xi) G(\tau_0 + t' - \xi) d\xi - 4\beta/3. \tag{12}$$

Therefore, when writing the Melnikov necessary condition for chaos, Eq. 12 may be used; there is no need to develop an explicit expression for $G_\epsilon(t)$.

For Eq. 9, $h(t) = 2^{1/2}\,\mathrm{sech}t\,\tanh t$. It follows immediately from Eqs. 10 and 12

$$M(t) = -4\beta/3 + 2^{1/2}\gamma F(t) \tag{13}$$

$$F(t) \approx \sum_{n=-\ell}^{\ell} a_n\{-\mathrm{sech}[(n+\alpha)t_1 - t] + \mathrm{sech}[(n+\alpha-1)t_1 - t]\} \tag{14}$$

where $t = \tau_0 + t'$, and ℓ is sufficiently large. The area under the curve $h(t)$ in a half-plane is $2^{1/2}$. It follows from the definition of $F(t)$ that $-2 < F(t) < 2$ (the integral in Eq. 14 yields $F(t) = 2$ if $\alpha = 0$, $a_n = 1$ for all n such that $t > 0$ and $a_n = -1$ for all n such that $t < 0$). Since the necessary condition for chaos (and, therefore, the necessary condition for escapes) is that $M(t)$ have simple zeros, it follows from Eq. 13 that chaos cannot occur if $F(t)$ does not reach the zero line $(4\beta/3)(2^{1/2}\gamma)$, or

$$F(t) < 0.9428\beta/\gamma. \tag{15}$$

Since $|F(t)| < 2$, chaos cannot occur if the following remarkably simple criterion

$$\gamma/\beta < 0.471 \tag{16}$$

is satisified. Figures 1a and 1b show time history realizations for dichotomous noise with parameters $t_1 = 1.0$, $\epsilon = 0.1$, $\beta = 1.5$ and, respectively, $\gamma/\beta = 0.469 < 0.471$, $\gamma/\beta = 1.887$. The motion of Fig. 1a is confined to one well. Its irregularity is due to the stochastic nature of the excitation. The chaotic motion of Fig. 1b is similar to chaotic motions induced in the standard Duffing-Holmes oscillator by harmonic or quasiperiodic excitation. Its irregularity is due to both the chaotic nature of the motion and the stochastic nature of the excitation. Sensitivity to initial conditions (i.e., the positivity of the largest Lyapounov exponent) was verified numerically for the motion of Fig. 1b.

3.3 Melnikov-based Lower Bounds for Mean Escape Time and for Probability of Non-occurrence of Escapes During a Specified Time Interval. Effective Melnikov Frequencies

Escapes from preferred regions associated with the potential wells are due to chaotic transport across the pseudoseparatrix. The transport is effected by the turnstile lobes of the system's intersecting stable and unstable manifolds.

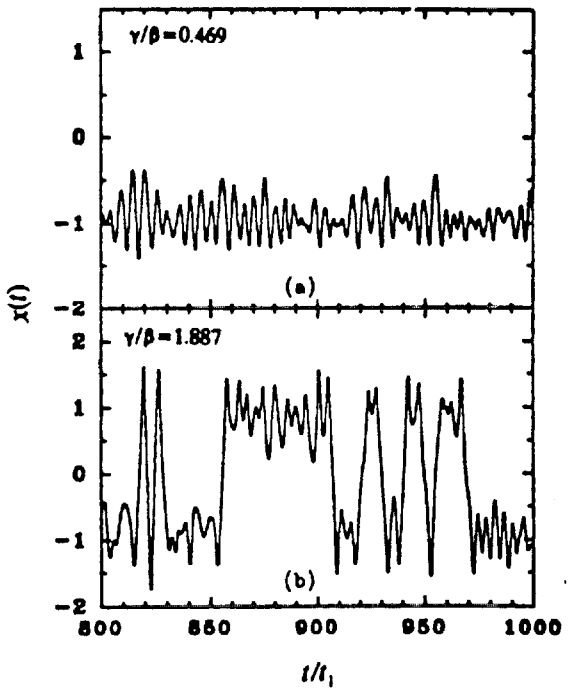

FIGURE 1. (a) Non-chaotic and (b) chaotic time histories x(t), induced by dichotomous noise.

On average no transport across the pseudoseparatrix can occur during a time interval smaller than the mean time between consecutive zero upcrossings of the Melnikov process, denoted τ_u. Therefore, *the mean time between consecutive zero upcrossings τ_u of the Melnikov process is a lower bound for the system's mean time of escape from a* well τ_e. Franaszek et al. (1997) present results which show that, for small perturbations by either Gaussian and dichotomous noise, this lower bound is weak.

We consider the system (9) and assume that $G(t)$ is a *Gaussian* process. The Melnikov process induced by white or colored Gaussian noise is Gaussian with mean, spectral density and standard deviation $-k$, $2\pi\Psi_M(\omega)$ and σ_M, respectively. The mean time between consecutive zero upcrossings for the Melnikov process is

$$\tau_u = \nu^{-1} \exp(\kappa^2/2) \tag{17}$$

$$\nu = (1/2\pi)\{[\int_0^\infty \omega^2\Psi_M(\omega)d\omega]/[\int_0^\infty \Psi_M(\omega)d\omega]\}^{1/2}, \qquad \kappa=k/\sigma_M \tag{18a,b}$$

(Rice, 1954, p. 193). We now consider Melnikov-based bounds for probabilities of no escape during a specified time interval. Provided that the escapes are rare events, the probability that there will no zero upcrossings of the Melnikov process during a time interval $T \ll \tau_u$ can be closely approximated by the Poisson distribution with average rate of arrival τ_u^{-1} and a number of upcrossing event occurrences during the interval T equal to zero, that is,

$$p_M(0,T)=\exp(-T/\tau_u) \tag{19}$$

The probability $p_M(0,T)$ is an approximate lower bound for the probability that no escapes from a well will occur during the interval T. The probability that there will be at least one zero upcrossing of the Melnikov process during the interval T is

$$p_{M,T}=1-\exp(-T/\tau_u) \tag{20}$$

The probability $p_{M,T}$ is an approximate upper bound for the probability that escapes from a well will occur during the interval T. Since, if the escapes are rare events, τ_u is a weak bound, so are $p_M(0,T)$ and $p_{M,T}$. Even though the upper bound is very weak for small perturbations, it may be useful in some applications. We remark that, for systems for which escapes would be undesirable, the upper bound $p_{M,T}$ has the advantage of being an estimate on the safe side.

In addition to providing lower bounds τ_u for the mean escape time τ_e, the Melnikov approach can be useful for qualitative assessments concerning the effect on τ_e of the spectral density of the excitation. Results of numerical simulations that provide useful insights into this effect are shown in Franaszek and Simiu (1995).

3.4 Slowly Varying Systems

Following Wiggins and Holmes (1987, 1988), Wiggins and Shaw (1988), who studied the case of periodic excitation, and Simiu (1996), who extended their work to systems with quasiperiodic and stochastic excitation, we review in this section the Melnikov necessary condition for chaotic behavior of the following class of slowly varying systems:

$$\begin{aligned} \dot{x} &= \frac{\partial}{\partial y} H(x,y,z) + \epsilon g_1(x,y,z,t;\mu) \\ \dot{y} &= -\frac{\partial}{\partial x} H(x,y,z) + \epsilon g_2(x,y,z,t;\mu) \\ \dot{z} &= \epsilon g_3(x,y,z,t;\mu) \end{aligned} \tag{21}$$

where ϵ is small, the right-hand side is C^r differentiable ($r \geq 2$), $H(x,y,z)$ is a Hamiltonian with parameter z, μ is a vector of parameters, and g_i ($i = 1,2,3$) are time periodic, quasiperiodic, or stochastic perturbation functions. It is shown in Wiggins and Holmes (1987, 1988) that the Melnikov function for the harmonically excited system is

$$M(t_0) = \int_{-\infty}^{\infty} \nabla H(q_0^{z_0}(t_0)).g(q_0^{z_0}(t,t+t_0)dt - \partial H(\Gamma(z_0))/\partial z \int_{-\infty}^{\infty} g_3(q_0^{z_0}(t,t+t_0)dt, \tag{22}$$

where $\nabla H = \{\partial H(q_0)/\partial x, \partial H(q_0)/\partial y, \partial H(q_0)/\partial y\}$, $g = [g_1, g_2, g_3]$, and $q_0^{z_0}(t)$ is the unperturbed homoclinic orbit connecting the hyperbolic fixed point of the unperturbed system at elevation z_0 to itself. The same expression can be easily shown to hold if the excitation is quasiperiodic or stochastic (Simiu, 1996). From Eq. 22 it follows that the Melnikov process can be interpreted as the sum of the outputs of three linear filters with inputs g_1, g_2 and g_3, respectively. Therefore means, spectral densities, and variances of Melnikov processes induced by additive or multiplicative stochastic excitations may be obtained. If $M(t_0)$ has simple zeros at some time $t = t_0$, for sufficiently small ϵ the stable and unstable manifolds of the perturbed system intersect transversely. By virtue of generalizations of the Smale-Birkhoff theorems chaos is possible in this case. If $M(t_0) \neq 0$ for all t_0, then the stable and unstable manifolds do not intersect and chaos cannot occur.

4. Along-shore Currents Induced by Randomly Fluctuating Wind over a Corrugated Ocean Floor

We consider a simple model of mesoscale wind-induced alongshore ocean flow over a continental margin with variable bottom topography. The model was developed by Allen et al. (1991) for the case of forcing by surface stresses fluctuating harmonically in time. Simiu (1996) extended the model for the more realistic case of stochastic forcing, and

compared results obtained for harmonic and stochastic forcing.

4.1 Offshore Flow Model. Wind Fluctuations and Wind Stresses. Melnikov Process

Averaging of the alongshore momentum equation over a wavelength of the corrugations yields for the model flow the nondimensional equations (21), where x is the basic nondimensional alongshore velocity, $y=\delta\phi_2$, $z=\frac{1}{2}x^2-x+\delta\phi_1$, $\delta=\delta'/(R_oD)$, δ' is the dimensional amplitude of the ocean floor corrugations, D is the depth scale, L is the length scale, R_o is the Rossby number,

$$g_1=-rx+\tau_o+\tau(t),\quad g_2=-ry,\quad g_3=-rz-\tfrac{1}{2}rx^2+(x-1)[\tau_o+\tau(t)] \qquad (23a,b,c)$$

$$H(x,y,z)=\tfrac{1}{2}y^2+zx+\tfrac{1}{2}(\omega_o^2-z)x^2-\tfrac{1}{2}x^3+(1/8)x^4,\quad \omega_o^2=1+\delta^2, \qquad (24)$$

$\epsilon r=\delta_E/2R_oD$ is a friction coefficient related to the eddy viscosity of the ocean flow, $\epsilon\tau_o$ and $\epsilon\tau(t)$ are, respectively, the steady and fluctuating wind stress divided by the wind stress scale τ_*, and δ_E is the depth of the ocean's bottom Ekman layer, assumed to be independent of the wind stresses (Allen et al., 1991). We consider the spectrum of the horizontal wind velocity fluctuations developed by Van der Hoven (1957). The spectrum (Fig. 2) has three main portions: one portion with a peak at a period of about 4 days, a second portion, known as the spectral gap, having negligible energy and extending over periods of about 5 hrs to 3 min, and a third portion, with a peak at a period of about 1 min, where fluctuations have relatively small spatial coherence and therefore have a negligible overall effect at the scale of our problem (Simiu and Scanlan, 1996). The units of $\Psi_u(\omega)$ are m^2/s^2 . For the spectrum of Fig. 2 the standard deviation of the wind velocity fluctuations $u(t)$ is $\sigma_u \approx 1.33$ m/s.

Under certain reasonable simplifications with respect to the wind structure (Simiu, 1996) we may assume that the spectral density of the wind stresses at the ocean surface

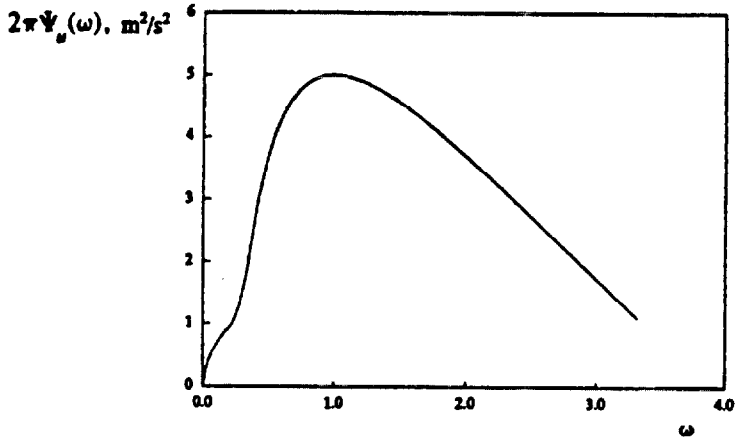

FIGURE 2. Spectral density of wind speed fluctuations.

is approximately proportional to $2\pi\Psi_u(\omega)$. We then write $\epsilon^2\gamma^2[2\pi\Psi_o(\omega)] \approx \epsilon^2\gamma^2[2\pi\Psi_u(\omega)/\sigma_u^2]$, where $\epsilon\gamma$ is the standard deviation of the wind stresses $\epsilon\tau(t) \approx \epsilon\gamma G(t)$, and the standard deviation of $G(t)$ is unity. Assuming the wind velocity fluctuations are Gaussian, it follows from the assumed proportionality between the fluctuating winds and the surface stresses that the latter are also Gaussian.

The Melnikov process is

$$M(t) = rC_1 + \int_{-\infty}^{\infty} g(\xi)\tau(\xi+t)d\xi \tag{25}$$

where $g(\xi)$ is a linear filter whose transfer function is $jC_2(\omega)$ [$j=(-1)^{1/2}$] (i.e., $C_2(\omega)$ is the Melnikov scale factor). Expressions for C_1 and C_2 are given by Allen et al. (1991). The expectation and variance of the Melnikov process are

$$E[M(t)] = rC_1 \tag{26}$$

$$\mathrm{Var}[M(t)] = \frac{\gamma^2}{2\pi}\int_0^{\infty} C_2^2(\omega)[2\pi\Psi_o(\omega)]d\omega. \tag{27}$$

4.2 Example

We consider the case, studied by Allen et al. (1991) for harmonic excitation, $\delta=0.3003$, $r_o/r=3.236\times10^{-3}$. The unperturbed system has the fixed points {0,0}, {1.236,0} and {1.764,0}. Calculations yield $C_1^+=2.524$, $C_1^-=-7.076$, where the superscripts $-$ and $+$ indicate the left- and right-hand side well, and

$$C_2^+(\omega) = -4.8\sinh(2.064\omega)/\sinh(5.5\omega), \quad C_2^-(\omega) = -4.8\sinh(3.436\omega)/\sinh(5.5\omega) \tag{28a,b}$$

For harmonic forcing $\epsilon\tau(t)=\epsilon(2)^{1/2}\gamma\cos(\omega t)$ with $\omega = 1$ (a case examined by Allen et al. (1991) and assumed therein to correspond to a dimensional time $T_{\mu k} \approx 4$ days), $C_2^+ = -0.152$, $C_2^- = -0.609$, and the necessary condition for escapes from the left well is satisfied for $\gamma/r > 8.22$, where $\epsilon\gamma$ is the standard deviation of the harmonic forcing.

This criterion may be misleading if the forcing is actually random with $\gamma/r=8.22$ or even smaller. Consider the forcing with spectrum $\epsilon^2\gamma^2[2\pi\Psi_o(\omega)]$, where $\epsilon\gamma$ now denotes the standard deviation of the srochastic forcing. Figures 3a and 3b show, respectively, the square of the Melnikov scale factor, $[C_2^-(\omega)]^2$, and the spectral density of the Melnikov process for $\gamma=1$, $2\pi\Psi_{Mo-}(\omega) = [C_2^-(\omega)]^2[2\pi\Psi_o(\omega)]$. The transfer function reduces the spectral components with frequencies $\omega > 1$ or so, and amplifies lower frequency components. Equation 18a applied to $2\pi\Psi_{Mo-}(\omega)$ and $2\pi\Psi_{Mo+}(\omega)$ yields $\nu^-=0.0702$ and $\nu^+=0.0534$, respectively. The standard deviations of the Melnikov process are $\sigma_{M+} = 0.359\gamma$ and $\sigma_{M-} = 0.778\gamma$, respectively, so $\kappa_- = |E[M_-]/\sigma_{M-}| = 9.1r/\gamma$ and $\kappa_+ = |E[M_+]/\sigma_{M+}| = 7.03r/\gamma$. We assume $\gamma/r<8.22$, say, $\gamma/r=4$, so $\kappa_-=2.273$ and

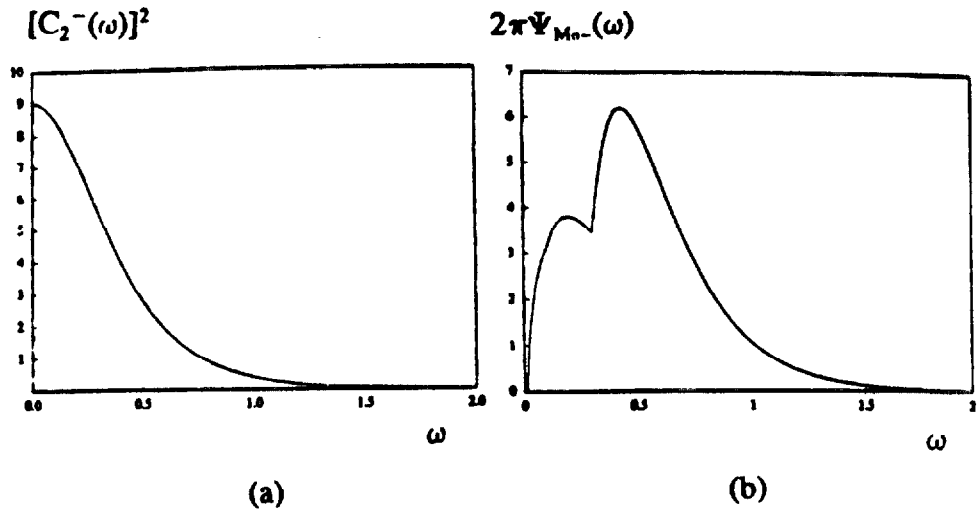

FIGURE 3. (a) Square of Melnikov scale factor, $[C_2^-(\omega)]^2$; (b) spectral density $2\pi\Psi_{Mo-}(\omega)$.

$\kappa_+=1.76$. From Eq. 17, $\tau_M(\kappa_-)=188.6$ (i.e., $188.6 \times 4/(2\pi)=119.7$ days) and $\tau_M(\kappa_+)=88.5$ (56.3 days) (the left well being larger than the right well). A lower bound for the probability that no escapes will occur from the left well during a time interval $T=1$ month (i.e., 47.1 nondimensional time units) is $p_{M,T-=1mo}=0.78$ (Eq.19). For the right well $p_{M,T+=1mo}=0.59$.

Suppose a decision would hinge on whether the probability that the motion will not escape from the larger well is at least 0.75 during one month. In our case the lower bound $p_{M,T-=1mo}=0.78$ would provide a conservative basis for such a decision.

5. Snap-through of Continuous Buckled Column With Distributed Random Load

In this section we illustrate the use of the Melnikov approach to obtain criteria on the occurrence of noise-induced jumps in a spatially-extended dynamical system (i.e., a system governed by a partial differential equation with space and time coordinates). The system chosen for this illustration is a buckled column with continuous mass, subjected to a transverse continuously distributed force that varies randomly with time. The force may be due, for example, to seismic motion, pressures induced by air flow turbulence, or effects arising in hydrodynamical systems.

For a deterministic counterpart of our problem -- a buckled column with uniform mechanical properties over its length, subjected to a transverse uniformly distributed load varying harmonically in time -- a Melnikov-based necessary condition for the occurrence of snap-through was obtained by Holmes and Marsden (1981). This condition is used as building block for the extension of the Melnikov approach to the case of random transverse loading (Franaszek and Simiu, 1996b).

Assume that (a) the mechanical properties of the column are uniform over its length,

(b) the behavior of the material is linearly elastic, (c) following the initial, static deformation of the column due to buckling the distance between the column supports is fixed, and (d) the column deformations are sufficiently small that, in the Taylor expansion of the projection of the elemental deformed column length on the line joining the column supports, terms of power higher than two can be neglected. The equation of the column is then (Holmes and Marsden, 1981)

$$z_{tt} + z_{yyyy} + \{\Gamma - \xi \int_0^1 z_y^2(\zeta,t)d\zeta\}z_{yy} = \epsilon\{R(y,t) - \beta z_t\} \tag{29a}$$

$$R(y,t) = \gamma(y)\cos(\omega_o t) + \rho(y)G(t) \tag{29b}$$

where $z(y,t)=Z(Y,\tau)/\Delta$ is the dimensionless deflection, Z is the deflection at time τ, Y is the coordinate along the column length ℓ, $y=Y/\ell$, $\Delta=Z_o(\ell/2)$ is the static deflection of the column $Z_o(Y)$ at coordinate $Y=\ell/2$, t and τ are the dimensionless and dimensional time, respectively, $\Gamma=P_o\ell^2/EI$, E is Young's modulus, I is the moment of inertia of the column cross-section,

$$P_o=P_{cr}+[EA/2\ell]\int_0^\ell (dZ_o/dY)^2dY, \tag{29c}$$

and $P_{cr}=k\pi^2EI/\ell^2$ is Euler's critical buckling load. For additional notations, see Franaszek and Simiu (1996b). The case of harmonic forcing, that is, $\rho(y)\equiv 0$, was studied by Holmes and Marsden (1981), who obtained the result

$$M(t_o) = k_1\beta+[\alpha_{\tau o1}/2+2\gamma_o/\pi]k_2(\omega_o)\sin(\omega_o t_o) \tag{30}$$

$$k_1 = -(2/3)\pi(\Gamma-\pi^2)^{1/2}, \quad k_2(\omega_o) = -(2\omega_o/\pi)/(\xi^{1/2})\text{sech}\{\omega_o/[2(\Gamma-\pi^2)^{1/2}]\}. \tag{31}$$

For sufficiently small ϵ, the stable and unstable manifolds of the perturbed system intersect transversely if $M(t_o)$ has simple zeros. The dynamics can then be chaotic.

We now consider the case of stochastic forcing and discuss briefly non-resonance conditions for this case. For harmonic forcing, the nonresonance condition $\omega_o^2 \neq -\lambda_j^2$ must be satisfied so that the solutions of the linearized counterparts of the Galerkin equations be of order $O(\epsilon)$, rather than $O(1)$. A similar requirement holds if the forcing is quasiperiodic. However, if the forcing is a stochastic process, then it has components over a continuous range of frequencies, that is, it may also have elemental components with frequencies equal to the natural frequencies of the system. In this case, for white or colored noise, it can be shown that the solutions are $O(\epsilon^\zeta)$, $\zeta<1$ (for white noise $\zeta=0.5$, see, e.g., Meirovich, 1967, p. 501). For sufficiently small ϵ the solutions will therefore be as small as desired, and nonresonance conditions are not required for Melnikov theory to be applicable. Also, if the noise is dichotomous, the probability that its spectral density

will have a given discrete component is zero, and nonresonance conditions are again not required. However, if $\rho(y)\neq 0$ and $\gamma(y)\neq 0$, nonresonance conditions must be satisfied for the harmonic forcing with frequency ω_0.

For stochastic forcing the Melnikov process has the same form as for the harmonic excitation case. If $\gamma(y)\equiv 0$ and $G(t)$ is *Gaussian* with spectrum $2\pi\Psi_0(\omega)$, the Melnikov process is Gaussian with spectral density, mean, and variance

$$2\pi\Psi_M(\omega)=2\pi\Psi_0(\omega)k_2^2(\omega), \qquad E[M]=k_1\beta, \tag{32a,b}$$

$$\mathrm{Var}[M]=(\alpha_{\rho 1}/2+2\rho_0/\pi)^2\int_{-\infty}^{\infty}\Psi_0(\omega)k_2^2(\omega)d\omega. \tag{32c}$$

Equations 32 may be used to estimate lower bounds for the mean time between snap-through events and for the probability that no snap-through occurs during an interval T. For dichotomous noise, it can be shown that the necessary condition for the occurrence of snap-through is $\rho_0>\rho_{0,\mathrm{crit}}=\pi^3\xi\beta/12$. The condition $\rho_0>\rho_{0,\mathrm{crit}}$ guarantees the non-occurrence of snap-through. For a numerical example, see Franaszek and Simiu (1996b).

6. Melnikov-based Open-Loop Control of Noise-induced Escapes

We consider the system

$$\dot{x}_1=x_2 \tag{33a}$$

$$\dot{x}_2=-V'+\epsilon[\gamma G(t)-\beta x_2-\alpha G_c(t)] \tag{33b}$$

where $\epsilon,\gamma,\beta,\alpha>0$ and ϵ is sufficiently small for Melnikov theory to be approximately valid. $\epsilon\gamma G(t)$ and $-\epsilon\alpha G_c(t)$ are the exciting force and the control force, respectively, and $G(t)$ is a stationary, ergodic stochastic process with unit variance and spectrum $2\pi\Psi_0(\omega)$.

The mean time of escape from a well τ_e can be reduced by adding a suitable control force. A trivial choice of the open-loop control force would be $G_c(t)\equiv G(t)$, $\alpha<\gamma$. For this trivial choice the ratio q between the average power of the control force and the average power of the excitation force is α^2/γ^2. Our objective is to obtain open-loop control forces that would achieve reductions of the system's mean escape rate comparable to those achieved by the trivial control, but more efficiently, that is, with a decreased ratio q. The proposed approach uses the fact that the shape of the Melnikov scale factor is nonuniform and exponentially decaying so that it indicates which excitation frequencies are effective or ineffective in inducing escapes. Instead of $G_c(t)\equiv G(t)$, it would be more efficient to apply a control force obtained from the process $G(t)$ by filtering out from the latter the frequency components that do not contribute significantly to the spectral density of the uncontrolled system's Melnikov process. The advantage of this approach over the trivial approach $G_c(t)\equiv G(t)$ is that it can achieve, with less power, a comparable reduction of the system's mean escape rate.

Simiu and Franaszek (1995, 1997) report numerical simulations which show that controls that use the information contained in the Melnikov scale factor can stabilize efficiently a system with random excitation. The degree to which this can be accomplished in practice depends upon the system under consideration (i.e., its Melnikov characteristics), the spectral density of the excitation, and the characteristics of the filters used to obtain the control force. For an approach to open-loop control based on the flux factor see Frey and Simiu (1996) and Frey (1996).

7. Stochastic Resonance

For a class of multistable systems with noise and a periodic signal, the improvement of the signal-to-noise ratio (SNR) achieved by increasing the noise intensity is known as stochastic resonance (SR) (or, as it will be referred to here, classical SR)

The essence of the physical mechanism underlying classical SR can be described as follows (McNamara and Wiesenfeld, 1989). Consider the motion in a bistable double-well potential of a lightly damped particle subjected to stochastic excitation and a harmonic excitation (i.e., a signal) with low frequency ω_0. The signal is assumed to have small enough amplitude that, by itself (i.e., in the absence of the stochastic excitation), it is unable to move the particle from one well to another. We denote the characteristic rate, that is, the escape rate from a well under the combined effects of the periodic excitation and the noise, by $\alpha=2\pi n_{tot}/T_{tot}$, where n_{tot} is the total number of exits from a well during the time interval T_{tot}. We consider the behavior of the system as we increase the noise while the signal amplitude and frequency are unchanged. For zero noise, $\alpha=0$, as noted earlier. For very small noise we have $\alpha<\omega_0$. As the noise increases, the ordinate of the spectral density of the output noise at the frequency ω_0, denoted $P_n(\omega_0)$, and the characteristic rate α increase. Experimental and analytical studies show that, until $\alpha\approx\omega_0$, a cooperative effect (i.e., a synchronization-like phenomenon), occurs wherein the signal output power $P(\omega_0)$ increases as the noise intensity increases. Remarkably, the increase of $P(\omega_0)$ with noise is faster than that of $P_n(\omega_0)$. This results in an enhancement of the SNR. The synchronization-like phenomenon plays a key role in the mechanism just described.

Melnikov theory yields qualitative results on the basis of which useful inferences can be made on the behavior of systems exhibiting stochastic resonance. Basically, we use the fact that for a wide class of systems, deterministic and stochastic excitations play qualitatively equivalent roles in inducing chaotic motions with escapes over a potential barrier, the motions being in both cases topologically conjugate to a shift map. This fact suggested the extension of SR approaches beyond classical SR. Franaszek and Simiu (1996a) showed that the SNR can alternatively be improved by keeping the noise unchanged and adding a deterministic excitation selected in accordance with Melnikov theory, rather than by increasing the noise. They also presented qualitative arguments and results of numerical simulations according to which this extension (1) significantly improves our ability to enhance SNR, (2) broadens the range of phenomena explainable by SR, and (3) allows the development of effective practical devices for enhancing SNR. Also, since Melnikov theory provides information on excitation frequencies that are effective in increasing a system's characteristic rate, the chaotic dynamics approach

makes it possible to assess the role of the excitation's spectral density in the enhancement of the SNR, a problem of interest in classical SR for which other available approaches can be unwieldy.

We review briefly the principle of a nonlinear transducing device for improving a signal's SNR was proposed proposed by Franaszek and Simiu (1996a). Consider a signal for which the SNR is unsatisfactory. The signal and the attendant noise – from which we filter out components well separated from the signal, that is, components with frequencies exceeding, say, three times the signal frequency – are used to excite the transducing device, consisting for example of a Duffing-Holmes oscillator. The SNR of the output will in general be poor, but under certain conditions it can be improved by the addition of a harmonic excitation with frequency equal or close to the frequency of the Melnikov scale factor's peak. The role of the added harmonic excitation is to bring about a chaotic motion with characteristic rate close to the signal frequency. To illustrate the

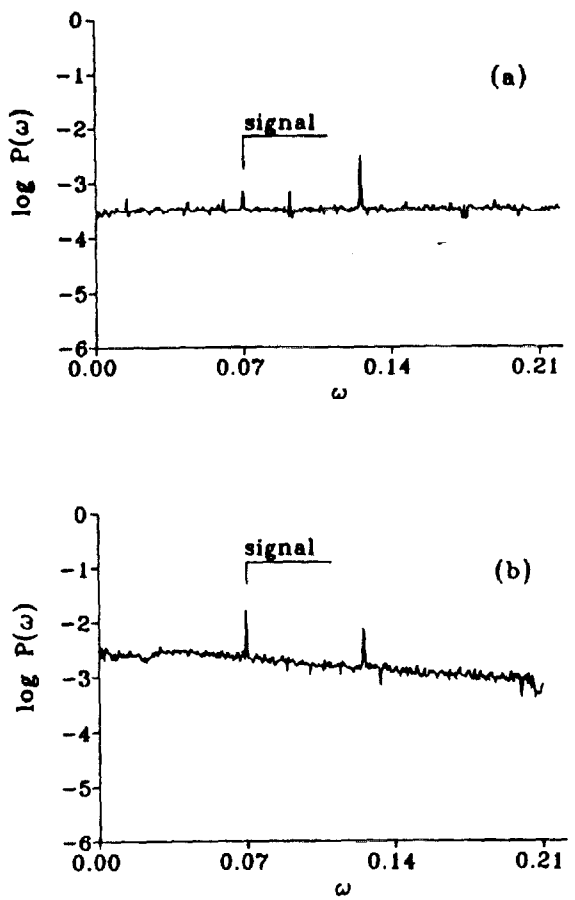

FIGURE 4. Averaged power spectra of (a) input consisting of stochastic excitation, harmonic signal with frequency $\omega_0 = 0.069$, and additional harmonic excitation with frequency $\omega_a = 1.1$; (b) output of transducing device (logarithms in base 10).

principle of the device, we show in Fig. 4a the spectrum of a signal $A_0\sin(\omega t)$, $A_0=0.05$, $\omega_0=0.069$ in the presence of noise broadband white noise $\gamma G(t)$, $\beta=0.25$ and $\gamma^2=0.36$. Using a low passband filter, we filter out the noise components with frequencies larger than three times the frequency of the signal. The signal and the noise left after the filtering (i.e., the noise $\gamma G(t)H(3\omega_0)$, where H denotes the Heaviside step function) are used as input to a standard Duffing-Holmes oscillator. For $A_a=0$ the SNR of the output is not better than the input SNR. However, by subjecting the nonlinear system to the additional excitation $A_a\sin(\omega_a t)$ ($A_a=0.23$ and $\omega_a=1.1$) we obtain the result with a considerably enhanced spectrum at the signal frequency shown in Fig. 4b.

8. Modeling of Auditory Nerve Fibers

The auditory nerve fiber is a natural device of interest to both neurophysiologists and signal processing engineers. Experiments have established two basic features of its dynamics. First, mean firing rates produced by harmonic excitation in the presence of weak noise are largest for excitation frequencies contained in a relatively narrow "best" interval; for frequencies outside that interval mean firing rates decrease and, for both low and high frequencies, become vanishingly small (Rose et al., 1967) (Fig. 5). Second, white or nearly white noise excitation results in multimodal interspike interval histograms (ISIH's) with modes approximately equal to integer multiples of the period corresponding to the nerve fiber's "best" frequency (Ruggiero, 1973) (Fig. 6). (For any given experiment an ISIH represents the number of occurrences of firings as a function of the time interval separating them.)

The Fitzhugh-Nagumo (FHN) model appears to be unable to reproduce these two dynamical features. According to Hochmair-Desoyer et al. (1984), in the absence of noise the FHN model predicts correctly that, as the excitation frequency increases beyond the "best" frequencies, the amplitude of the harmonic signal needed to cause firing increases sharply. However, the model fails to predict a similarly sharp increase for excitation frequencies lower than the "best" frequencies (Fig. 7). In the presence of noise the disagreement between typical FHN model predictions and the experimental results of Rose et al. (1967) appears to be even stronger (Hochmair-Desoyer et al., 1984, p. 561). Also, according to Longtin (1993), for nearly white noise excitation the FHN model yields a unimodal ISIH (Fig. 8), in disagreement with Ruggiero's experiments.

This section describes an asymmetric bistable model which, in contrast to the FHN model, reproduces the experimentally observed dynamical features noted earlier. The model is also consistent with experimental results on response patterns for excitation by two harmonics in the presence of spontaneous activity. Its performance can be interpreted transparently in terms of Melnikov theory.

8.1 Asymmetric Bistable Model of Auditory Nerve Fiber Response

The proposed model for the response of the auditory nerve fiber is the equation

$$\ddot{x}=-V'(x)+\epsilon(x)[\gamma_{01}\cos(\omega_{01}t)+\gamma_{02}\cos(\omega_{02}t)+\sigma G(t)-\beta\dot{x}], \tag{34}$$

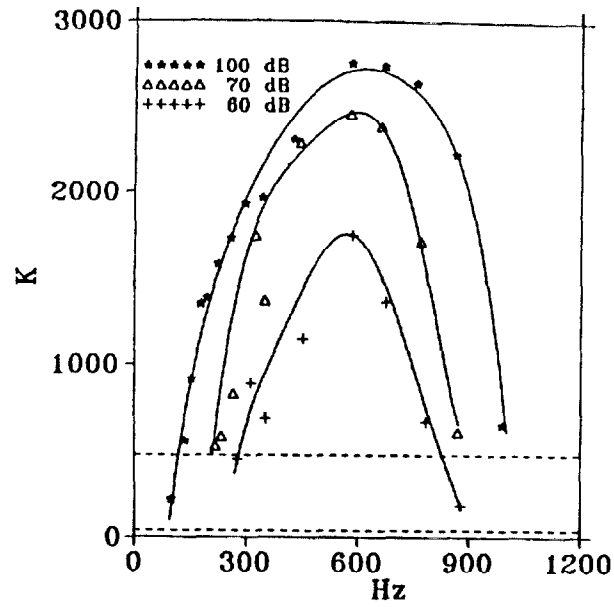

FIGURE 5. Dependence of K on frequency and amplitude of harmonic excitation. (K=number of spikes observed in 20 s for harmonically excited auditory nerve fiber in squirrel monkey.) Interrupted lines indicate levels of spontaneous firing. (After Rose et al., 1967)

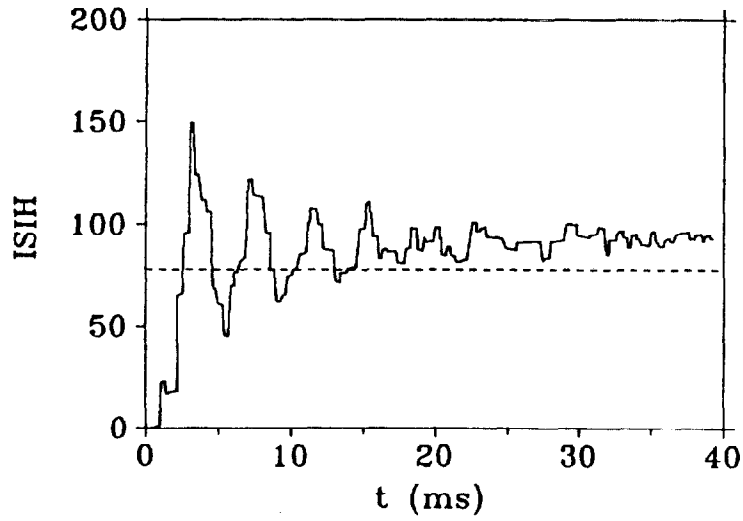

FIGURE 6. Interspike interval histogram for response to white noise of auditory nerve fiber in squirrel monkey. Interrupted line indicates level of spontaneous firing rate. Modes are approximately equal to integer multiples of the "best" period . (After Ruggiero, 1973.)

$$\epsilon(x) \equiv 1 - H(x) \tag{35}$$

where $H(x)$ is the unit step (Heaviside) function, and

$$V(x) = \alpha(x)(-x^2/2 + x^4/4) \tag{36}$$

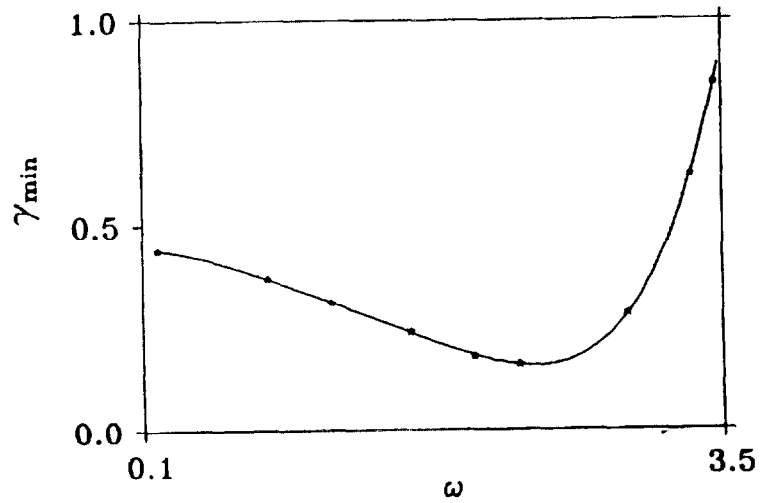

FIGURE 7. Dependence of minimum amplitude needed to produce firings, γ_{min}, on frequency of the harmonic excitation in the absence of noise, as modeled by Fitzhugh-Nagumo equation. Horizontal scale is logarithmic. (After Hochmayr-Desoyer, 1984.)

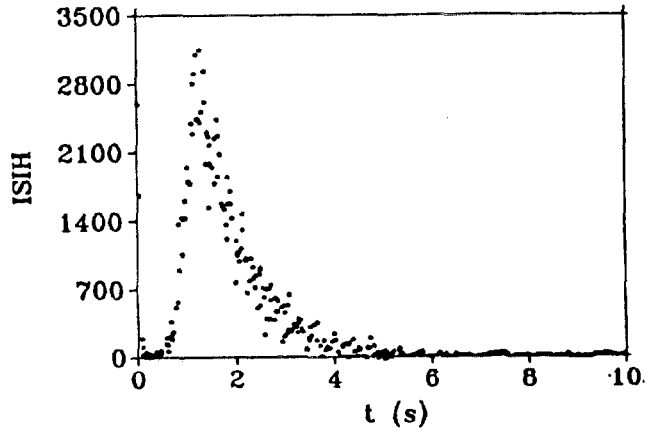

FIGURE 8. Interspike interval histogram for response induced by white noise as simulated by the Fitzhugh-Nagumo equation. (After Longtin, 1993.)

is a strongly asymmetric, modified version of the Duffing-Holmes potential. In Eq. 3 $\alpha(x)=1$ for $x\leq 0$ and $\alpha(x)=\alpha_o$ for $x>0$, where $\alpha_o \gg 1$. (It can be verified easily th $V'(0)=0$.) The potential $V(x)$ is depicted in Fig. 9a for $\alpha_o=49$.

For the perturbed system chaotic transport – escapes – can occur only in the hal plane $x\leq 0$, since owing to the form of Eq.34 the system remains unperturbed for $x>0$ The Melnikov necessary condition for chaos must then be satisfied for the shallowe potential well of Fig. 9a. The corresponding Melnikov scale factor is

$$S(\omega)=(2)^{1/2}\pi\omega\,\mathrm{sech}(\pi\omega/2) \tag{37}$$

(Fig. 10). Figure 10 shows that for our model, just as for the experiments of Rose et al (1967), excitation components become increasingly ineffective in inducing chaos an therefore escapes as their frequencies are farther away from a "best" frequency. (Th term "escapes" corresponds in our model to the the neurophysiological term "firings."

Throughout this section it is assumed that the two-sided spectral density of $G(t)$ i

$$2\pi\Psi_o(\omega)=2c/(1+c^2\omega^2) \tag{38}$$

in which $c=0.02$, that is, the spectral density varies slowly with frequency and i therefore a close approximation of white noise.

Equation 34 is a bistable system whose unperturbed counterpart has homoclinic orbits Therefore, depending upon its parameters, our model of the auditory nerve fiber ca experience stochastic resonance. Although experimental results on the stochasti resonance of some types neurons are available, to our knowledge none have bee reported for the auditory nerve fiber.

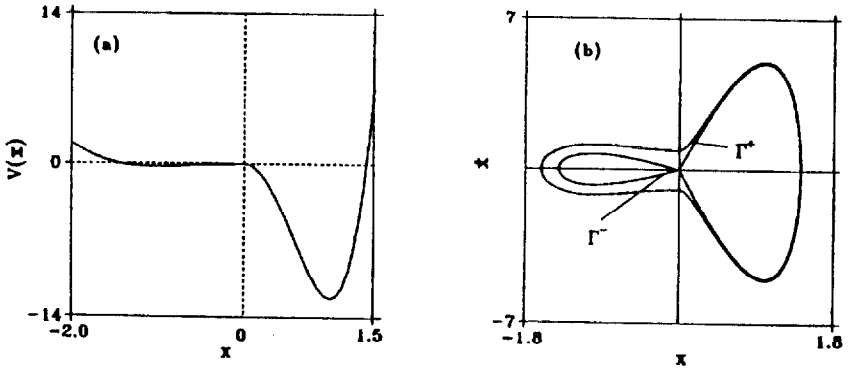

FIGURE 9. (a) Potential $V(x)$ ($\alpha_o=49$); (b) phase plane diagram showing homoclinic orbits and an orbi visiting the half-planes $x\leq 0$ and $x>0$.

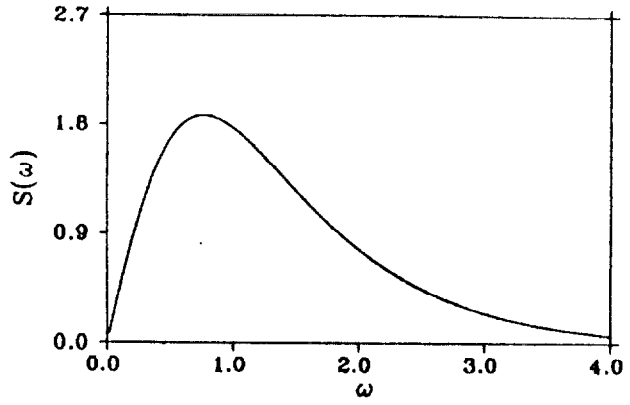

FIGURE 10. Melnikov scale factor $S(\omega)$.

8.2 Chaotic Response to Harmonic and Stochastic Excitation

We now describe a typical chaotic motion pattern for our model. Denote by $\mathbf{R}^-$ the perturbed system's counterpart of the core enclosed by the homoclinic orbit (separatrix) Γ^-. Following an escape from $\mathbf{R}^-$, firing occurs and the motion evolves outside the core enclosed by the impermeable separatrix Γ^+ until its return to the half-plane $x \leq 0$. Chaotic transport into $\mathbf{R}^-$, followed by another escape (firing) can then occur again. A typical time history of this type of motion is shown in Fig. 11, based on Eq. 34, the potential function of Fig. 9a, the parameter values $\gamma_{o1}=0.11$, $\gamma_{o2}=0$, $\beta=0.16$, $\sigma=0.005$, $\omega_{o1}=1.0$, and the spectral density of the process $G(t)$ given by Eq. 35. The weak noise used in the simulations is intended to mimic the noise inducing the fiber's spontaneous activity. As noted by Rose et al. (1967, p. 776), the responses may exhibit multiple firings in response to a stimulating cycle, rather than a single discharge. A double firing can be seen in Fig. 11 at $t/T_{o1} \approx 80$.

8.3 Dependence of Mean Firing Rate on Frequency of Harmonic Excitation

In view of the dependence of the model response on the Melnikov scale factor (Fig. 10), response patterns are similar qualitatively to those obtained experimentally (Fig. 5). We assume $\gamma_{o2}=0$, $\beta=0.16$, $\sigma=0.005$, and the spectral density of $G(t)$ given by Eq. 38. We show in Fig. 12 the dependence of the mean firing rate r on the frequency ω_{o1} for two amplitudes of the harmonic forcing: $\gamma_{o1}=0.12$ and $\gamma_{o1}=0.10$. For any given frequency, the larger amplitude causes a larger firing rate. For both amplitudes the harmonic excitation is seen to be increasingly ineffective in producing firings as the excitation frequencies are farther away from either end of a relatively narrow "best" frequency interval. The dependence of the mean firing rate on amplitude and frequency is indeed

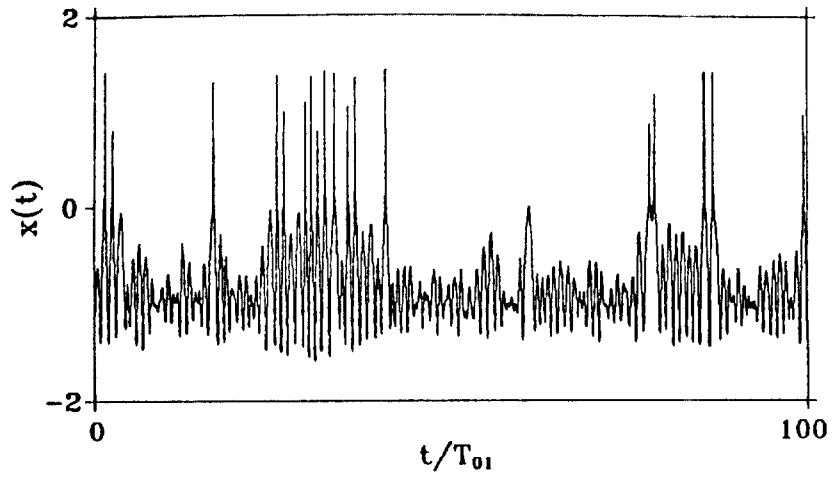

FIGURE 11. Time history of motion induced by harmonic excitation in the presence of noise (Eq. 34). ($T_{o1}=2\pi/\omega_{o1}$.)

qualitatively similar to the experimental results of Fig. 5. The results of Fig. 12 are consistent with Melnikov theory only in a qualitative sense since the peak of the Melnikov scale factor (Fig. 10) does not coincide with the peaks of the mean rate plots. This is due to second order effects resulting from the relatively large perturbation.

8.4 Interspike Interval Histograms

We assume again $\gamma_{o2}=0$, $\beta=0.16$, $\sigma=0.005$, and the spectral density of $G(t)$ given by Eq. 38. Figures 13a-c show ISIH's for $\gamma_{o1}=0.12$ and $\omega_{o1}=1.25$, $\omega_{o1}=1.05$, and $\omega_{o1}=0.8$, respectively. The "best" frequency in this case is $\omega_{best}\approx 1.1$ (Fig.), that is, Figs. 13a-c correspond, respectively, to harmonic excitation frequencies higher than, approximately equal to, and lower than the "best" frequency. The period of the harmonic excitation is $T_{01}=2\pi/\omega_{o1}$. The ISIH's of Figs. 13a-c were obtained by simulation from Eq. 34. They are multimodal and agree qualitatively with ISIH's based on experiments (Rose et al, 1967). Both for the experiments and for Figs. 13a-c the peaks in the ISIH's are grouped around the integer multiples of the period of the harmonic excitation. Nevertheless, the firing is aperiodic, which is consistent with the fact that the motions are chaotic. The preference for the forcing period and its integer multiples reflects the large spectral ordinate of the response at the forcing frequency (which is typical of the harmonically forced Duffing oscillator (Guckenheimer and Holmes, 1986, p.88]), and the corresponding subharmonics. Note the presence in Fig. 13 of components with periods shorter than the dominant period. As was pointed out by Rose et al (1967, p.776), these components reflect the existence of multiple firings.

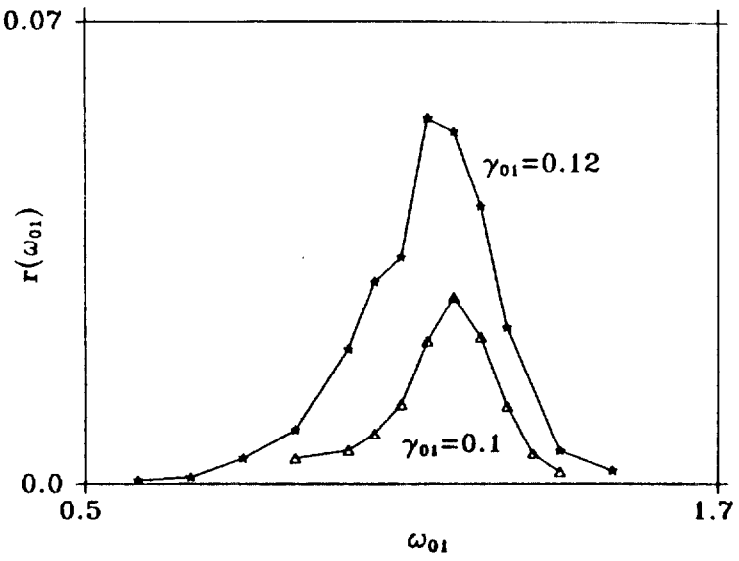

FIGURE 12. Dependence of firing rate r on harmonic excitation frequency for two excitation amplitudes γ_{01}, simulated by Eq. 34 with harmonic excitation in the presence of noise.

ISIH's based on the FHN model (Longtin, 1993) are, like the results of Fig. 13a-c, in qualitative agreement with the experimental results of Rose et al (1967). However, for excitation by nearly white noise the FHN model does not appear to be in agreement with the experimental results of Ruggiero (1973): the IHIS's obtained from those experiments of are multimodal, whereas those based on the FHN model were found to be unimodal, as shown in Fig. 7 (Longtin, 1993). In contrast, simulations based on Eq. 34 agree well with the experimental results of Ruggiero (1973)]. This is illustrated by Fig. 13d, which shows a typical ISIH based on Eq. 34 with the same parameters as those of Figs. 13a-c, except that $\gamma_{01}=0$ and $\sigma=0.035$, that is, the only excitation is stochastic. The ISIH is multimodal with periodicities closely related to the "best" frequency. The results of Fig. 13d are consistent with Melnikov theory since components with the "best" frequencies – frequencies closely related to the frequency of the Melnikov scale factor's peak – are the most effective in inducing escapes. The behavior of the system can therefore be expected to be determined by those components and their integer multiples.

Melnikov theory as applied to our model is also in qualitative agreement with results of experiments in which auditory nerve fibers were excited by two harmonic functions in the presence of spontaneous activity (Hind et al., 1967). In those experiments the frequency of one of the harmonic excitations, denoted ω_{01}, was close to the "best" frequency ω_{best}, while for the second harmonic $\omega_{02}<\omega_{best}$, so that its effectiveness in inducing firing was relatively weak. The results of Hind et al. (1967) indicated that the ISIH's are multimodal, with basic period $T_{01}=2\pi/\omega_{01}$ or $T_{02}=2\pi/\omega_{02}$ according as the ratio $\eta=\gamma_{01}/\gamma_{02}$ of the amplitudes corresponding to ω_{01} and ω_{02} is

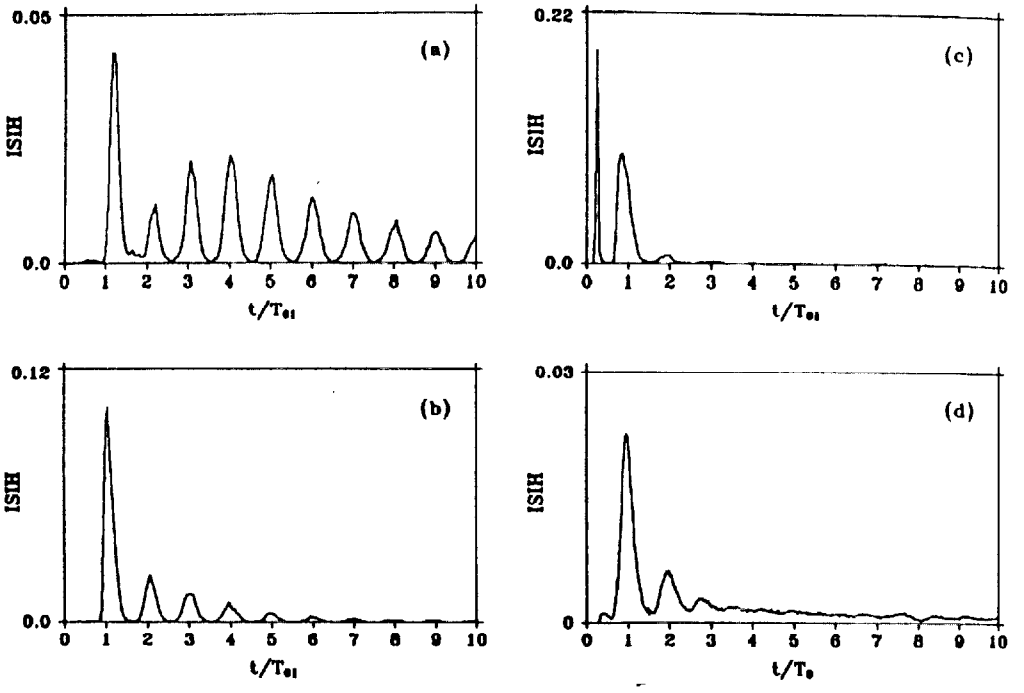

FIGURE 13. Interspike interval histograms simulated from Eq. 34: (a-c) Harmonic excitation in the presence of noise for excitation frequency larger than, approximately equal to, and smaller than the "best" frequency, respectively; (d) excitation by nearly white noise. T_{01} and T_0 denote the period of the harmonic excitation and the period corresponding to the "best" frequency, respectively.

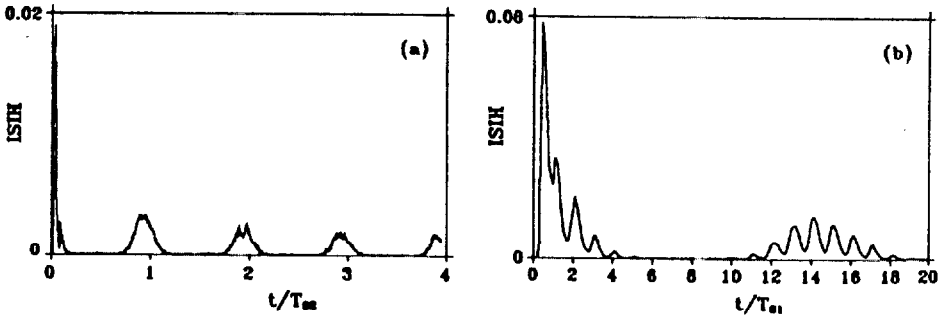

FIGURE 14. Interspike interval histograms simulated from Eq. 34 for excitation by two hamonics in the presence of noise. Dominant frequencies are controlled by: (a) excitation with inefficient frequency but relatively large amplitude, (b) excitation with frequency close to "best" frequency.

condition from chaos. Even though $S(\omega_{o1})$ is larger than $S(\omega_{o2})$, if the ratio η is sufficiently small the motion can be dominated by the harmonic with inefficient frequency. That this is indeed the case is shown by the simulations of Fig. a,b, for which $\omega_{o1}=1.0\approx\omega_{best}$, $\omega_{o2}=0.06\ll\omega_{best}$, $\beta=0.25$, and $\sigma=0.0075$. For Fig. 14a, $\gamma_{o1}=0.01$ and $\gamma_{o2}=0.3$ ($\eta=0.033$). Apart from the two peaks at $t/T_{o2}\ll 1$, which are ascribed to multiple firings, the spikes are grouped around the period T_{o2} and its integer multiples. For Fig. b, $\gamma_{o1}=0.1$, $\gamma_{o2}=0.16$, and period T_{o1} controls.

Acknowledgements

The work summarized in this paper was supported in part by the Ocean Engineering Division of the Office of Naval Research, grants N00014-94-0028 and N00014-94-0284.

References

J.S. Allen, R.M. Samelson, and P.A. Newberger, *J. Fluid Mech.* **226** 511 (1991).
D.K. Arrowsmith and C.M. Place, *An Introduction to Dynamical Systems*, Cambridge University Press, Cambridge (1990).
D. Beigie, A. Leonard, and S. Wiggins, *Nonlinearity* 4 775 (1991).
M. Franaszek, C. Hagwood, E. Simiu and Y. Sivathanu, Y. 7th Intern. Conf. on Structural Safey and Reliability, ICOSSAR '97, Kyoto (1997).
M. Franaszek and Simiu, E., *Physics Lett.* 205 137 (1995).
M. Franaszek and E. Simiu, *Physical Rev.* E 54 1288 (1996a).
M. Franaszek and E. Simiu, *Int. J. Non-linear Mech.*, 31 861 (1996b).
M. Frey, *IEEE Trans. Autom. Contr.* 216 (1996a).
M. Frey, *Proceedings, 7th ASCE Conf. Prob. Mechs. Struct. Reliab.*, D. Frangopol and M. Grigoriu (eds.), Amer. Soc. Civ. Engrs. (1996b).
M. Frey and E. Simiu, *Physica* D63 321 (1993).
M. Frey and E. Simiu, *Proc.,NATO Adv.Workshop, Spatio-Temporal Patterns in Nonequilibrium Complex Systems, P.* Cladis and P. Pally-Muhoray (eds.), Santa Fe Institute in the Sciences of Complexity, Addison-Wesley (1995).
M. Frey and E. Simiu, *Physica* D95 128 (1996).
J. Guckenheimer and P. Holmes, *Nonlinear Oscillations, Dynamical Systems, and Bifurcations of Vector Fields*, Springer-Verlag, New York (1986).
J.E. Hind, D.J. Anderson, J.F. Brugge and J.R. Rose, *J. Neurophysiol.* 30 794 (1967).
I.J. Hochmair-Desoyer, E.S. Hochmair, H. Motz and F. Rattay, *Neurosc.* 13 553 (1984).
P. Holmes and J. Marsden, *Arch. Ration. Mech. Anal.* 76 135 (1981).
A.Longtin, *J.Stat.Phys.* 70 309 (1993).
B. McNamara and K. Wiesenfeld *Physical Rev.* A 39 4854 (1989)..
S.O. Rice, S.O. in: *Selected Papers...*, A. Wax, ed., Dover, New York (1954).
J.R. Rose, J.F. Brugge, D. Anderson and J.E.Hind, *J.Neurophysiol.* 30 769 (1967)..
M.A. Ruggiero, *J. Neurophysiol.* 36 569 (1973).
E. Simiu, *J. Appl. Mech.* 63 429 (1996).

E. Simiu and M. Franaszek, *J. Dynam. Syst., Measurement & Control* (1997, in press).
E. Simiu and M. Franaszek, *IUTAM Symp. Adv. Nonl. Stoch. Mechs.*, A. Naess, A. and S. Krenk, Kluwer, Dordrecht (1996).
E. Simiu and M. Frey *Proc. Workshop on Fluctuations and Order: The New Synthesis*, M. Millonas (ed.), Springer-Verlag, N.Y. (1996a).
E. Simiu and M. Frey, *J. Eng. Mech.* **122** 263 (1996b).
E. Simiu and M. Grigoriu, *J. Offshore Mech. Arctic Eng.* **117** 166 (1995).
E. Simiu and R. Scanlan, *Wind Effects on Structures*, 3rd Ed., Wiley, New York (1996).
Y. Sivathanu, C. Hagwood, C. and E. Simiu, *Physical Rev.* **E52** 4669 (1995).
I. Van der Hoven, *J. Meteor.* **14** 160 1957).
F. Verhulst, *Nonlinear Differential Equations and Dynamical Systems*, Springer-Verlag, New York. (1990).
S. Wiggins, *Global Bifurcations and Chaos: Analytical Methods*, Springer, New York (1988)..
S. Wiggins, *Chaotic Transport in Dynamical Systems*, Springer. New York (1992).
S. Wiggins. and P. Holmes, "Homoclinic Orbits in Slowly Varying Oscillators," *SIAM J. Math. Anal.* **18** 612 (1987); Errata: **19** 1254 (1988).
Wiggins, S. and S.W. Shaw, *J. Appl. Mech.* **55** 959 (1988).